

First Passage Distance to Connectivity for Mobile Robots

Arjun Muralidharan and Yasamin Mostofi

Abstract—We consider a robot that needs to establish connectivity with a remote human operator (or with another robot) as it moves along a path. We are interested in answering the following question: how long would the robot move before it finds a connected spot? More specifically, we are interested in mathematically characterizing the PDF of the distance traveled before the robot gets connected, as a function of the underlying wireless channel parameters. We start with the case where multipath fading is negligible, and utilize the stochastic differential equation literature to derive the PDF of the distance traveled before connectivity, considering shadowing and path loss components of the channel. We then include the effect of multipath and carry out the analysis using stochastic dynamic programming. Finally, we confirm our theoretical derivations by running several simulations with real channel parameters and highlight interesting trends of the distance to connectivity.

I. INTRODUCTION

There has been a considerable interest in networks of unmanned vehicles in recent years. Such networks are envisioned to have a wide range of applications such as surveillance and emergency response [1], [2]. While unmanned vehicles are becoming more capable of autonomous operations, there still exist many tasks where they may need help from human operators [3]–[5]. For instance, consider the case where an unmanned vehicle is given an exploratory field mission. As it senses the environment more, it may need to contact the remote operator to transfer the gathered data, or to ask for help with interpreting the collected data. Thus, if it is not connected in its current spot, it needs to find a location that has a good connectivity to the remote operator to establish the communication. Furthermore, there will be several cases where an unmanned vehicle needs to get connected to another node. In this paper, we are then interested in answering the following question: “How long does the robot need to travel before it finds a connected spot?”. In other words, we are interested in mathematically characterizing the probability density function (PDF) of the distance to connectivity, as a function of the underlying channel parameters.

In general, connectivity plays a key role in the operation of unmanned vehicles as the nodes need to communicate among themselves as well as with the remote human operators. As such, considering both communication and motion planning issues has been a subject of several research papers in recent years. For instance, in [6], [7], the connectivity of a network

is maximized using the Fiedler eigenvalue of the underlying graph, while in [8], connectivity is optimized using a more realistic channel model and the performance metric for connectivity is taken to be the end-to-end BER of the system. In [1], [9]–[12], the authors propose communication-aware path planning strategies in order to accomplish certain sensing and communication tasks. In [13], the authors propose an optimal control framework for the co-optimization of communication and motion.

However, the problem of mathematically characterizing the statistics of the distance traveled before the robot gets connected has not been explored, which is the main motivation for this paper. We refer to this problem as **the first passage distance problem**, analogous to the concept of first passage time [14]. We then mathematically characterize the PDF of the first passage distance as a function of the underlying channel parameters of the environment, such as shadowing, path loss, and multipath fading parameters. The derivations of the paper can thus bring a foundational analytical understanding to the first passage distance and how different environments with different underlying parameters affect it. The analysis can further help with the operation on the field and the design of robotic paths. For instance, the five underlying parameters of the channel can typically be measured based on very few channel samples in the environment, either online or from prior operations. Thus, the robot can assess the statistics of its distance to connectivity, using our derivations, when on a field mission. Furthermore, the derivations can be used to explicitly co-optimize and design robotic sensing and path planning as part of future work. We finally emphasize that the derivations of the paper are applicable to both cases of trying to establish communication with human operators and trying to establish communication with another robot.

The paper is organized as follows. In Section II, we formally define our problem and briefly summarize the model for the spatial variations of the channel. In Section III, we analyze the statistics to connectivity while ignoring the multipath component, which could be of interest when the robot looks for an area of good connectivity as opposed to a single spot. In this case, we utilize the stochastic differential equation (SDE) literature in our derivations. In Section IV, we include the effect of multipath in the analysis, and show how the first passage PDF can be efficiently derived using stochastic dynamic programming. Finally, in Section V, the theoretical characterizations are validated with simulation results using channel parameters obtained from real channel data in downtown San Francisco.

This work is supported in part by NSF NeTS award 1321171 and in part by NSF RI award 1619376.

The authors are with the Department of Electrical and Computer Engineering, University of California Santa Barbara, Santa Barbara, CA 93106, USA email: {arjunm, ymostofi}@ece.ucsb.edu.

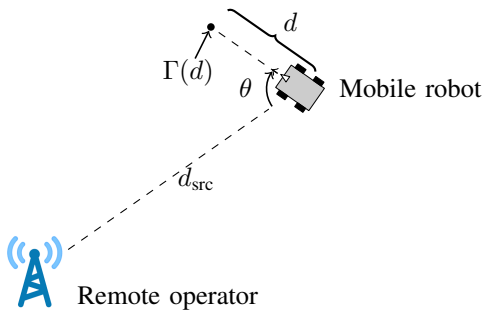


Fig. 1: An example of the considered scenario.

II. PROBLEM SETUP

Consider a robot situated at a distance d_{src} from a remote operator or from another robot to which it needs to be connected and moving in the direction specified by the angle θ , as shown in Fig. 1. The angle θ is measured clockwise with respect to the line segment connecting the remote operator and the robot, as can be seen in Fig. 1, and denotes the direction of travel chosen by the robot. In order for the robot to successfully connect with the remote operator, the receptions need to satisfy the Quality of Service (QoS) requirement such as a target Bit Error Rate, which in turn results in a minimum required received Signal to Noise Ratio, or equivalently a minimum required channel power, given a fixed transmission power. We denote this minimum required received channel power as γ_{th} in this paper. This paper then asks the following question: “What is the distance traveled by the robot before it gets connected to the remote human operator?”. More specifically, we are interested in mathematically characterizing the probability density function (PDF) of this distance as a function of the underlying channel parameters of the operation environment, such as path loss, shadowing and multipath fading parameters, and given d_{src} and θ . We note that while we assume that the robot travels on a straight line in this paper, the analysis can be extended to any given trajectory as part of future work.

A. Channel Model [15]

In the communication literature, channel power is well modeled as a multi-scale random process with three major dynamics: path loss, shadowing and multipath fading. Let $\Gamma(q)$ represent the received channel power (in the dB domain) at location $q \in \mathbb{R}^2$ with the remote operator located at the origin. It can then be expressed as $\Gamma(q) = \gamma^{\text{PL}}(q) + \Gamma^{\text{SH}}(q) + \Gamma^{\text{MP}}(q)$ where $\gamma^{\text{PL}}(q) = K_{\text{dB}} - 10n_{\text{PL}} \log_{10} \|q\|$ is the distance-dependent path loss with n_{PL} representing the path loss exponent, and Γ^{SH} and Γ^{MP} are random variables denoting the impact of shadowing and multipath respectively (in dB). The multipath component or small-scale fading represents fluctuations in the channel power on the order of a wavelength, while the shadowing component or large-scale fading represents fluctuations of the channel power after the signal is locally averaged over multipath, thus reflecting the impact of larger objects such as blocking buildings. $\Gamma^{\text{SH}}(q)$ is best modeled as a Gaussian random process with an exponential spatial correlation, i.e., $\mathbb{E}\{\Gamma^{\text{SH}}(q_1)\Gamma^{\text{SH}}(q_2)\} =$

$\sigma_{\text{SH}}^2 e^{-\|q_1 - q_2\|/\beta_{\text{SH}}}$ where σ_{SH}^2 is the shadowing power and β_{SH} is the decorrelation distance [15]. As for multipath, a number of distributions such as Nakagami, Rician and lognormal have been found to be a good fit (in the linear domain) [15], [16].

Since the robot moves along a straight line, we are only interested in the statistics of the channel power along this line. Let d be the distance traveled by the robot along direction θ . With a slight abuse of notation, in the rest of the paper we let $\Gamma(d)$ represent the channel power when the robot is at distance d along direction θ , as marked in Fig. 1. We thus have $\Gamma(d) = \gamma^{\text{PL}}(d) + \Gamma^{\text{SH}}(d) + \Gamma^{\text{MP}}(d)$, where

$$\gamma^{\text{PL}}(d) = K_{\text{dB}} - 5n_{\text{PL}} \log_{10}(d_{\text{src}}^2 + d^2 - 2d_{\text{src}}d \cos \theta), \quad (1)$$

and $\Gamma^{\text{SH}}(d)$ is a zero mean Gaussian process with the spatial correlation of $\mathbb{E}\{\Gamma^{\text{SH}}(d_1)\Gamma^{\text{SH}}(d_2)\} = \sigma_{\text{SH}}^2 e^{-(d_2 - d_1)/\beta_{\text{SH}}}$, with $d_2 \geq d_1$. Note that $\Gamma(d)$ is also a function of d_{src} and θ . We drop $\Gamma(d)$'s dependency on them in the notation as the analysis of the paper is carried out for a fixed d_{src} and θ .

As we shall show in the next section, $\Gamma^{\text{SH}}(d)$ becomes an Ornstein-Uhlenbeck process, one of the most studied types of Gauss-Markov processes [17]–[20]. Ornstein-Uhlenbeck process appears in many practical scenarios, such as Brownian motion, financial stock markets, or neuronal firing [18], [19], and thus has been heavily studied in the literature. In this paper, we shall utilize this rich literature [20], [21] to mathematically characterize the first passage distance to connectivity for a mobile robot.

III. CHARACTERIZING THE FIRST PASSAGE DISTANCE WITHOUT CONSIDERING MULTIPATH - STOCHASTIC DIFFERENTIAL EQUATION ANALYSIS [20], [21]

In this section we start our analysis by ignoring the multipath and only considering the shadowing and path loss components of the channel, i.e., we want $\Gamma(d) = \gamma^{\text{PL}}(d) + \Gamma^{\text{SH}}(d)$ to be above γ_{th} . This assumption allows us to better analyze and understand the first passage distance using stochastic differential equations, and paves the way towards our most general characterization of the next section, which includes multipath as well. Moreover, the analysis also has practical values of its own, and would be relevant to the case where the robot is interested in finding a general area of good connectivity as opposed to a single good spot. In the rest of the paper, we will use the abbreviation FPD to refer to the First Passage Distance. We next establish that the corresponding channel power, $\Gamma(d) = \gamma^{\text{PL}}(d) + \Gamma^{\text{SH}}(d)$, is a Gaussian Markov (Gauss-Markov) process. We begin by summarizing the definitions of a Gaussian process and a Markov process.

Definition 1 (Gaussian Process [22]): A stochastic process $\{X(t) : t \in T\}$, where T is an index set, is a Gaussian process, if any finite number of samples have a joint Gaussian distribution, i.e., $(X(t_1), X(t_2), \dots, X(t_k))$ is a Gaussian random vector for all $t_1, \dots, t_k \in T$ and for all k .

A Gaussian process is completely specified by its mean function $m(t) = \mathbb{E}[X(t)]$ and its covariance function $C(s, t) = \mathbb{E}\{(X(s) - m(s))(X(t) - m(t))\}$. We use the notation $X \sim \mathcal{GP}(m, C)$ to denote the underlying process.

Definition 2 (Markov Process [23]): A process $X(t)$ is Markov if $\Pr(X(t_n) \leq x_n | X(t_{n-1}), \dots, X(t_1)) = \Pr(X(t_n) \leq x_n | X(t_{n-1}))$, for all n and for all $t_n \geq t_{n-1} \geq \dots \geq t_1$, where $\Pr(\cdot)$ denotes the probability of the argument.

Definition 3 (Gauss-Markov Process [24]): A stochastic process is Gauss-Markov if it satisfies the requirements of both a Gaussian process and a Markov process.

We next state a lemma that shows when a Gaussian process is also Markov, which we shall utilize to prove that the channel power $\Gamma(d)$ is Gauss-Markov.

Lemma 1: A Gaussian process $X \sim \mathcal{GP}(m, C)$ is Markov if and only if $C(s, u) = C(s, t)C(t, u)/C(t, t)$, for all $u \geq t \geq s$.

Proof: See [25] for the proof. ■

Corollary 1: The channel power $\Gamma(d)$ is a Gauss-Markov process.

Proof: $\Gamma \sim \mathcal{GP}(\gamma^{\text{PL}}, C_\Gamma)$ is a Gaussian process with mean function $\gamma^{\text{PL}}(d)$ and covariance $C_\Gamma(s, u) = \sigma_{\text{SH}}^2 e^{-(u-s)/\beta_{\text{SH}}}$. This covariance function satisfies $C_\Gamma(s, t)C_\Gamma(t, u)/C_\Gamma(t, t) = \sigma_{\text{SH}}^2 e^{-(u-t)-(t-s)/\beta_{\text{SH}}} = C_\Gamma(s, u)$, for $u \geq t \geq s$, which concludes the proof using Lemma 1. ■

Remark 1 (see [20]): The Ornstein-Uhlenbeck process $O \sim \mathcal{GP}(0, C_O)$ is a Gauss-Markov process with the covariance function $C_O(s, u) = \sigma^2 e^{-(u-s)/\beta}$, where $\sigma \geq 0$ and $\beta \geq 0$ are constants. Thus, we can see that the channel power $\Gamma(d)$ is the sum of an Ornstein-Uhlenbeck process ($\Gamma^{\text{SH}}(d)$) and a mean function (path loss function $\gamma^{\text{PL}}(d)$).¹

In order to gain more insight into the stochastic process $\Gamma(d)$, we next discuss the transition PDF $f(\gamma, d|\eta, l) = \frac{\partial}{\partial \gamma} \Pr(\Gamma(d) < \gamma | \Gamma(l) = \eta)$, where $d \geq l$, as well as the stochastic differential equation governing $\Gamma(d)$, both of which we shall subsequently use in our characterization of the PDF of the FPD.

A. The Underlying Stochastic Differential Equation

The transition PDF $f(\gamma, d|\eta, l)$ characterizes the distribution of $\Gamma(d)$ given $\Gamma(l) = \eta$. It is straightforward to show that it is a normal density characterized by mean and variance of

$$\begin{aligned} \mathbb{E}[\Gamma(d)|\Gamma(l) = \eta] &= \gamma^{\text{PL}}(d) + e^{-(d-l)/\beta_{\text{SH}}}(\eta - \gamma^{\text{PL}}(l)) \\ \text{Var}[\Gamma(d)|\Gamma(l) = \eta] &= \sigma_{\text{SH}}^2(1 - e^{-2(d-l)/\beta_{\text{SH}}}). \end{aligned} \quad (2)$$

The transition PDF explicitly shows the spatial dependence of the channel power $\Gamma(d)$. As stated in [21], $f(\gamma, d|\eta, l)$ satisfies the partial differential equation known as the Forward Fokker-Planck equation:²

$$\begin{aligned} \frac{\partial}{\partial d} f(\gamma, d|\eta, l) &= -\frac{\partial}{\partial \gamma} [A(\gamma, d)f(\gamma, d|\eta, l)] \\ &\quad + \frac{1}{2} \frac{\partial^2}{\partial \gamma^2} [Bf(\gamma, d|\eta, l)], \end{aligned} \quad (3)$$

¹Note that $\Gamma(d)$ and $\Gamma^{\text{SH}}(d)$ are both Gauss-Markov processes and that $\Gamma^{\text{SH}}(d)$ is in particular an Ornstein-Uhlenbeck process.

²The Fokker-Planck equation of [21] is stated for a general Gauss-Markov process. Here we adapted it for our specific Gauss-Markov process $\Gamma(d)$.

with the associated initial condition of $f(\gamma, l|\eta, l) = \delta(\gamma - \eta)$, where $A(\gamma, d) = \frac{d\gamma^{\text{PL}}(d)}{dd} - \frac{(\gamma - \gamma^{\text{PL}}(d))}{\beta_{\text{SH}}}$, $B = (2\sigma_{\text{SH}}^2)/\beta_{\text{SH}}$ and $\gamma^{\text{PL}}(d)$ is as stated in (1), with its derivative:

$$\frac{d\gamma^{\text{PL}}(d)}{dd} = -10n_{\text{PL}} \log_{10}(e) \frac{d - d_{\text{src}} \cos \theta}{d_{\text{src}}^2 + d^2 - 2d_{\text{src}}d \cos \theta}.$$

The Fokker-Planck equation shows the evolution of the probability density $f(\gamma, d|\eta, l)$ with the distance traveled d given $\Gamma(l) = \eta$.

Moreover, as shown in [20], the channel power $\Gamma(d)$ can be represented as a stochastic differential equation:³

$$d\Gamma(d) = A(\Gamma, d)dd + \sqrt{B}dW(d), \quad (4)$$

where $W(d)$ is the Wiener process and $A(\gamma, d)$ and B are as defined before.

Remark 2: In (3) and (4), $A(\gamma, d)$ and B are known as the drift and the diffusion components respectively. The drift $A(\gamma, d) = \frac{d\gamma^{\text{PL}}(d)}{dd} - \frac{(\gamma - \gamma^{\text{PL}}(d))}{\beta_{\text{SH}}}$ is a pull towards the mean, and the diffusion component $B = (2\sigma_{\text{SH}}^2)/\beta_{\text{SH}}$ is a function of the shadowing variance and the decorrelation distance. Then, in an increment Δd , we can think of the channel power spatially evolving with a deterministic rate $A(\gamma, d)$, in addition to a random Gaussian term with the variance $B\Delta d$.

Next, we utilize our established lemmas to derive the PDF of the FPD.

B. First passage distance

Consider the random variable $\mathcal{D}_{\gamma_0} = \inf_{d \geq 0} \{d : \Gamma(d) \geq \gamma_{\text{th}}\}$ where $\Gamma(0) = \gamma_0 < \gamma_{\text{th}}$. This denotes the first passage distance (FPD) of the process $\Gamma(d)$ to the connectivity threshold γ_{th} , with the initial value $\Gamma(0) = \gamma_0 < \gamma_{\text{th}}$. Further, let $g[d|\gamma_0] = \frac{\partial}{\partial d} \Pr(\mathcal{D}_{\gamma_0} < d)$ represent the PDF of the FPD. In the following theorem, we characterize this PDF.

Theorem 1: The PDF of FPD $g[d|\gamma_0]$ satisfies the following non-singular second-kind Volterra integral equation:

$$g[d|\gamma_0] = -2\Psi[d|\gamma_0, 0] + 2 \int_0^d g[l|\gamma_0] \Psi[d|\gamma_{\text{th}}, l] dl, \quad (5)$$

where $\gamma_0 < \gamma_{\text{th}}$ and

$$\begin{aligned} \Psi[d|\eta, l] &= \left\{ -\frac{1}{2} \frac{d\gamma^{\text{PL}}(d)}{dd} - \frac{\gamma_{\text{th}} - \gamma^{\text{PL}}(d)}{2\beta_{\text{SH}}} \frac{1 + e^{-2(d-l)/\beta_{\text{SH}}}}{1 - e^{-2(d-l)/\beta_{\text{SH}}}} \right. \\ &\quad \left. + \frac{\eta - \gamma^{\text{PL}}(l)}{\beta_{\text{SH}}} \frac{e^{-(d-l)/\beta_{\text{SH}}}}{1 - e^{-2(d-l)/\beta_{\text{SH}}}} \right\} f(\gamma_{\text{th}}, d|\eta, l). \end{aligned} \quad (6)$$

Proof: The proof is based on the fact that $\Gamma(d)$ is a Gauss-Markov process and utilizes the Fokker-Planck equation (3). The details are then adapted from Theorem 3.1 of [21] to our particular Gauss-Markov process. ■

\mathcal{D}_{γ_0} represents the FPD for a given initial value of $\Gamma(0) = \gamma_0$. In many scenarios, we are instead interested in characterizing the FPD for an initial state $\Gamma(0) = \Gamma_0$, which is a random variable bounded from above by γ_{th} (as

³Reference [20] provides the stochastic differential equation for the Ornstein-Uhlenbeck process, from which we can easily obtain (4).

opposed to a given value that is not connected), i.e., we are interested in characterizing the FPD when the starting position is not connected. This is known as the upcrossing FPD in the general first passage literature [21]. We next extend our analysis to derive the PDF of the upcrossing FPD. Let the PDF of Γ_0 be given by

$$\zeta_\epsilon(\gamma_0) = \begin{cases} \frac{f(\gamma_0, 0)}{\Pr(\Gamma(0) < \gamma_{\text{th}} - \epsilon)}, & \gamma_0 < \gamma_{\text{th}} - \epsilon \\ 0, & \gamma_0 \geq \gamma_{\text{th}} - \epsilon \end{cases},$$

where $\epsilon > 0$ is a fixed real number and $f(\gamma, d)$ is the PDF of $\Gamma(d)$. Let the random variable $\mathcal{D}_{\Gamma_0}^{(\epsilon)} = \inf_{d \geq 0} \{d : \Gamma(d) \geq \gamma_{\text{th}}\}$ denote the ϵ -upcrossing FPD of $\Gamma(d)$ to the boundary γ_{th} given the initial state $\Gamma(0) = \Gamma_0$. The ϵ -upcrossing FPD, $\mathcal{D}_{\Gamma_0}^{(\epsilon)}$, can be characterized as follows:

$$\Pr(\mathcal{D}_{\Gamma_0}^{(\epsilon)} < d) = \int_{-\infty}^{\gamma_{\text{th}} - \epsilon} \Pr(\mathcal{D}_{\gamma_0} < d) \zeta_\epsilon(\gamma_0) d\gamma_0,$$

where \mathcal{D}_{γ_0} is the FPD given the initial value $\Gamma(0) = \gamma_0$, as defined earlier. Moreover, the ϵ -upcrossing FPD density $g_u^{(\epsilon)}[d] = \frac{\partial}{\partial d} \Pr(\mathcal{D}_{\Gamma_0}^{(\epsilon)} < d)$ is similarly related to the FPD density $g[d|\gamma_0]$ as follows: $g_u^{(\epsilon)}[d] = \int_{-\infty}^{\gamma_{\text{th}} - \epsilon} g[d|\gamma_0] \zeta_\epsilon(\gamma_0) d\gamma_0$.

Remark 3: Note that we have required $\epsilon > 0$. This is due to the fact that the mathematical tools we shall utilize are not well-defined for $\gamma_0 = \gamma_{\text{th}}$. However, ϵ can be chosen arbitrarily small.

In the following theorem, we derive an expression for $g_u^{(\epsilon)}[d]$, the PDF of the ϵ -upcrossing FPD.

Theorem 2: The PDF of the ϵ -upcrossing FPD, $g_u^{(\epsilon)}[d]$, satisfies the following non-singular second-kind Volterra integral equation:

$$g_u^{(\epsilon)}[d] = -2\Psi_u^{(\epsilon)}[d] + 2 \int_0^d g_u^{(\epsilon)}[l] \Psi[d|\gamma_{\text{th}}, l] dl, \quad (7)$$

where $\Psi[d|\eta, l]$ is as defined in (6),

$$\Psi_u^{(\epsilon)}[d] = \frac{1}{2\Pr(\Gamma(0) < \gamma_{\text{th}} - \epsilon)} \left\{ -\frac{2\sigma_{\text{SH}}^2}{\beta_{\text{SH}}} e^{-d/\beta_{\text{SH}}} f(\gamma_{\text{th}} - \epsilon, 0) \right. \\ \times f[\gamma_{\text{th}}, d|\gamma_{\text{th}} - \epsilon, 0] + \frac{1}{2} f(\gamma_{\text{th}}, d)(1 + \text{Erf}[\phi_\epsilon(d)]) \\ \left. \times \left(-\frac{d\gamma^{\text{PL}}(d)}{dd} - \frac{1}{\beta_{\text{SH}}} [\gamma_{\text{th}} - \gamma^{\text{PL}}(d)] \right) \right\},$$

with $\text{Erf}(z) = \frac{2}{\sqrt{\pi}} \int_0^z e^{-t^2} dt$ representing the error function, and

$$\phi_\epsilon(d) = \frac{\gamma_{\text{th}} - \epsilon - \gamma^{\text{PL}}(0) - e^{-d/\beta_{\text{SH}}} (\gamma_{\text{th}} - \gamma^{\text{PL}}(d))}{\sqrt{2\sigma_{\text{SH}}^2 (1 - e^{-2d/\beta_{\text{SH}}})}}.$$

Proof: The proof is obtained by adapting Theorem 5.3 of [21] to our particular Gauss-Markov process form. ■

In terms of implementation, the functions $\Psi[d|\eta, l]$ and $\Psi_u^{(\epsilon)}[d]$ in Theorem 1 and Theorem 2 can be easily computed. The PDF of the FPD ($g[d|\gamma_0]$) and the PDF of the ϵ -upcrossing FPD ($g_u^{(\epsilon)}[d]$) can then be computed from the integral equations (5) and (7) respectively. In particular, Simpson rule provides the basis for an efficient iterative algorithm for evaluating these integrals (See Section 4 of [21]). We skip the details due to page limitations.

IV. CHARACTERIZING THE FIRST PASSAGE DISTANCE CONSIDERING MULTIPATH – STOCHASTIC DYNAMIC PROGRAMMING ANALYSIS

The previous section analyzed the first passage distance to the connectivity threshold when the multipath component was ignored. In this section, we show how to derive the FPD density in the presence of the multipath fading component, and for the most general channel model of $\Gamma(d) = \gamma^{\text{PL}}(d) + \Gamma^{\text{SH}}(d) + \Gamma^{\text{MP}}(d)$. In this case, the approach of Section III is not applicable anymore as we no longer deal with a Gauss-Markov process. Even if the multipath component was taken to be a Gauss-Markov process (which could be a valid model for some environments [16]), the resultant channel power would not be, as can be verified from Lemma 1.

Recall that we define connectivity as the event where $\Gamma(d) \geq \gamma_{\text{th}}$. The connectivity requirement is then given as $\Gamma(d) = \gamma^{\text{PL}}(d) + \Gamma^{\text{SH}}(d) + \Gamma^{\text{MP}}(d) \geq \gamma_{\text{th}}$, considering all the channel components. In this section, we assume that the robot measures the channel along the chosen straight path in discrete steps of size Δ . We assume that Δ is such that the multipath random variable is uncorrelated at the distance Δ apart (this is a realistic assumption as multipath decorrelates fast [15], [26], [27]). We then index the channel power and shadowing components accordingly, i.e., let $\Gamma_k = \Gamma(k\Delta)$ and $\Gamma_k^{\text{SH}} = \Gamma^{\text{SH}}(k\Delta)$. The probability of failure of connectivity at the end of N steps (given the initial failure of connectivity) can then be written as

$$\Pr(\Gamma_1, \Gamma_2, \dots, \Gamma_N < \gamma_{\text{th}} | \Gamma_0 < \gamma_{\text{th}}) \\ = \int_{\gamma_1, \dots, \gamma_N < \gamma_{\text{th}}} p(\gamma_1, \dots, \gamma_N | \Gamma_0 < \gamma_{\text{th}}) d\gamma_1 \dots d\gamma_N, \quad (8)$$

where $p(\gamma_1, \dots, \gamma_N | \Gamma_0 < \gamma_{\text{th}})$ is the conditional joint density function of $\Gamma_1, \dots, \Gamma_N$. Consider the computation of this integral, which is an integration in an N dimensional space. If we discretize the domain of Γ_k into M parts, then a direct computation would involve M^N computations, which is infeasible for high values of M and N . Instead, we show how this problem can be posed as a dynamic programming problem and efficiently solved with $N \times M$ operations.

As mentioned before, the robot measures the channel in discrete steps of size Δ . Let $d_k = k\Delta$ denote the distance when k steps are taken. Then, it can be shown, using (2), that the shadowing component is an autoregressive AR(1) process, the continuous analogue of which is the Ornstein-Uhlenbeck process:

$$\Gamma_{k+1}^{\text{SH}} = \rho \Gamma_k^{\text{SH}} + \sigma_{\text{SH}} \sqrt{1 - \rho^2} Z_k,$$

where $\rho = e^{-\Delta/\beta_{\text{SH}}}$ and Z_k are i.i.d. with a standard normal distribution. The conditional random variable $\Gamma_{k+1}^{\text{SH}} | \Gamma_k^{\text{SH}}$ is thus a Gaussian random variable with mean $\rho \Gamma_k^{\text{SH}}$ and variance $\sigma_{\text{SH}}^2 (1 - \rho^2)$.

We define our state at the k^{th} stage to be $s_k = (\gamma_k^{\text{SH}}, d_k) \in S_k$ where $S_k = \mathbb{R} \times \{k\Delta\}$. The transition dynamics of the state is then given by the stochastic kernel, $T_s(s_{k+1} | s_k) = T_{\gamma^{\text{SH}}}(\gamma_{k+1}^{\text{SH}} | \gamma_k^{\text{SH}}) = \mathcal{N}(\gamma_{k+1}^{\text{SH}}; \rho \gamma_k^{\text{SH}}, \sigma_{\text{SH}}^2 (1 - \rho^2))$, where

$\mathcal{N}(z; m, \sigma^2)$ is defined as the probability density function of variable z , which has a Gaussian distribution with mean m and variance σ^2 . Define the cost of state s_k of the k^{th} stage to be $c(s_k) = \int_{-\infty}^{\gamma_{\text{th}} - \gamma_{\text{PL}}(d_k) - \gamma_k^{\text{SH}}} f_{\text{MP, dB}}(\gamma^{\text{MP}}) d\gamma^{\text{MP}} = \Pr(\Gamma_k < \gamma_{\text{th}} | \Gamma_k^{\text{SH}} = \gamma_k^{\text{SH}})$, i.e., the probability of failure of connectivity given the state, where $f_{\text{MP, dB}}(\cdot)$ is the density function of the random variable Γ^{MP} .

Note that the desired probability of (8) can be expressed as

$$\begin{aligned} & \Pr(\Gamma_1, \dots, \Gamma_N < \gamma_{\text{th}} | \Gamma_0 < \gamma_{\text{th}}) \\ &= \frac{\int \Pr(\Gamma_0, \dots, \Gamma_N < \gamma_{\text{th}} | \Gamma_0^{\text{SH}} = \gamma_0^{\text{SH}}) f_{\Gamma_0^{\text{SH}}}(\gamma_0^{\text{SH}}) d\gamma_0^{\text{SH}}}{\Pr(\Gamma_0 < \gamma_{\text{th}})}, \end{aligned} \quad (9)$$

where $f_{\Gamma_0^{\text{SH}}}(\cdot) = \mathcal{N}(\cdot; 0, \sigma_{\text{SH}}^2)$ is the density function of Γ_0^{SH} . Moreover $\Pr(\Gamma_0, \dots, \Gamma_N < \gamma_{\text{th}} | \Gamma_0^{\text{SH}} = \gamma_0^{\text{SH}})$ can be expressed as

$$\begin{aligned} & \Pr(\Gamma_0, \Gamma_1, \dots, \Gamma_N < \gamma_{\text{th}} | \Gamma_0^{\text{SH}} = \gamma_0^{\text{SH}}) \\ &= \Pr(\Gamma_0 < \gamma_{\text{th}} | \Gamma_0^{\text{SH}} = \gamma_0^{\text{SH}}) \\ & \quad \times \int \dots \int \prod_{k=0}^{N-1} \Pr(\Gamma_{k+1} < \gamma_{\text{th}} | \Gamma_{k+1}^{\text{SH}} = \gamma_{k+1}^{\text{SH}}) \\ & \quad \quad \quad \times T_{\gamma^{\text{SH}}}(\gamma_{k+1}^{\text{SH}} | \gamma_k^{\text{SH}}) d\gamma_{k+1}^{\text{SH}} \\ &= c(s_0) \int_{S_1} \dots \int_{S_N} \prod_{k=0}^{N-1} c(s_{k+1}) T_s(s_{k+1} | s_k) ds_{k+1}. \end{aligned} \quad (10)$$

We next show how to compute (10) by applying stochastic dynamic programming. Define the set of functions $J_k : S_k \rightarrow \mathbb{R}$, as follows:

$$\begin{aligned} J_N(s_N = (\gamma_N^{\text{SH}}, d_N)) &= \Pr(\Gamma_N < \gamma_{\text{th}} | \Gamma_N^{\text{SH}} = \gamma_N^{\text{SH}}), \\ J_k(s_k = (\gamma_k^{\text{SH}}, d_k)) &= \Pr(\Gamma_k, \dots, \Gamma_N < \gamma_{\text{th}} | \Gamma_k^{\text{SH}} = \gamma_k^{\text{SH}}), \end{aligned} \quad \text{for } k = 0, \dots, N-1. \quad (11)$$

Note that by definition $\Pr(\Gamma_0, \dots, \Gamma_N < \gamma_{\text{th}} | \Gamma_0^{\text{SH}} = \gamma_0^{\text{SH}}) = J_0(\gamma_0^{\text{SH}}, d_0)$. In the following Lemma we show how to compute $J_0(\gamma_0^{\text{SH}}, d_0)$ through backward recursion.

Lemma 2: The functions $J_k : S_k \rightarrow \mathbb{R}$, for $k = 0, \dots, N-1$, of (11) can be computed by the following backward recursion:

$$J_k(s_k) = c(s_k) \int_{S_{k+1}} J_{k+1}(s_{k+1}) T_s(s_{k+1} | s_k) ds_{k+1},$$

initialized with $J_N(s_N) = c(s_N)$.

Proof: It can be seen that this clearly holds for $k = N$:

$$J_N(s_N) = \Pr(\Gamma_N < \gamma_{\text{th}} | \Gamma_N^{\text{SH}} = \gamma_N^{\text{SH}}) = c(s_N).$$

Using backward recursion starting at $k = N-1$, $J_k(s_k)$ can be expanded as

$$\begin{aligned} J_k(s_k) &= \Pr(\Gamma_k, \dots, \Gamma_N < \gamma_{\text{th}} | \Gamma_k^{\text{SH}} = \gamma_k^{\text{SH}}) \\ &= \Pr(\Gamma_k < \gamma_{\text{th}} | \Gamma_k^{\text{SH}} = \gamma_k^{\text{SH}}) \\ & \quad \times \int \Pr(\Gamma_{k+1}, \dots, \Gamma_N < \gamma_{\text{th}} | \Gamma_{k+1}^{\text{SH}} = \gamma_{k+1}^{\text{SH}}) \\ & \quad \quad \quad \times T_{\gamma^{\text{SH}}}(\gamma_{k+1}^{\text{SH}} | \gamma_k^{\text{SH}}) d\gamma_{k+1}^{\text{SH}} \\ &= c(s_k) \int_{S_{k+1}} J_{k+1}(s_{k+1}) T_s(s_{k+1} | s_k) ds_{k+1}, \end{aligned}$$

which concludes the proof. \blacksquare

Using Lemma 2, we can compute $J_0(\gamma_0^{\text{SH}}, d_0)$ which in turn is used to compute $\Pr(\Gamma_1, \dots, \Gamma_N < \gamma_{\text{th}} | \Gamma_0 < \gamma_{\text{th}})$ via (9).

Next, we use this result to calculate the first passage distance probability. Define the random variable $\mathcal{K} = \min_{k=1,2,\dots} \{k : \Gamma_k \geq \gamma_{\text{th}}, \Gamma_0 < \gamma_{\text{th}}\}$, which denotes the up-crossing first passage step to connectivity given that Γ_0 is restricted to lie below γ_{th} . Then,

$$\begin{aligned} \Pr(\mathcal{K} = k) &= \Pr(\Gamma_1, \dots, \Gamma_{k-1} < \gamma_{\text{th}}, \Gamma_k \geq \gamma_{\text{th}} | \Gamma_0 < \gamma_{\text{th}}) \\ &= \Pr(\Gamma_1, \dots, \Gamma_{k-1} < \gamma_{\text{th}} | \Gamma_0 < \gamma_{\text{th}}) \\ & \quad - \Pr(\Gamma_1, \dots, \Gamma_k < \gamma_{\text{th}} | \Gamma_0 < \gamma_{\text{th}}), \end{aligned}$$

where both terms on the right hand side can be obtained from our dynamic programming formulation using Lemma 2.

V. SIMULATION RESULTS

In this section, we validate the derivations of Sections III and IV in a simulation environment with real channel parameters. We also highlight interesting trends of the first passage distance statistics as a function of the distance to the remote operator, direction of travel and the channel parameters. The channel is generated using the channel model described in Section II-A, using parameters obtained from real channel measurements in downtown San Francisco [28]: $n_{\text{PL}} = 4.2$, $\sigma_{\text{SH}}^2 = 8.41$ and $\beta_{\text{SH}} = 12.92$ m. We impose a minimum required received SNR of 20 dB and the noise power is taken to be a realistic -100 dBmW. This corresponds to a minimum required received power of -80 dBmW. We take the transmit power to be 30 dBmW, which results in a channel power connectivity threshold of $\gamma_{\text{th}} = -110$ dB. We furthermore take $\epsilon = 0.1$ in the simulation results.

A. Results Without Considering Multipath

We first consider the case without multipath. Fig. 2 is a sample realization of the first passage distance for crossing the connectivity threshold. The figure also shows the mean of the channel, which is the path loss component.

Fig. 3 shows the PDF and CDF of the upcrossing FPD for $d_{\text{src}} = 500$ m, with the robot moving at the angle $\theta = \pi/4$ radian. The figure shows both the theoretical derivations as well as the result of brute-force simulations. It can be seen that our derived expressions matches the simulated ones well.

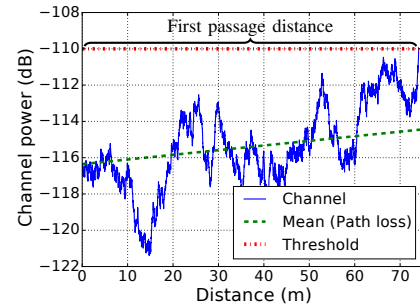


Fig. 2: A sample realization of the first passage distance for crossing the connectivity threshold.

When considering the first passage distance to connectivity, it should be noted that $D_{\Gamma_0}^\epsilon$ may not be a proper random

variable, i.e.⁴, $\Pr(\mathcal{D}_{\Gamma_0}^\epsilon < \infty) < 1$. To see how this may arise, consider the case when the robot moves away from the remote operator. In this case, it is reasonable to expect that with a finite probability the robot will never be connected to the remote operator, especially if it started far from the remote operator to begin with. Formally, let $P_{\text{conn},\infty} = \Pr(\mathcal{D}_{\Gamma_0}^\epsilon < \infty)$ denote the probability of connectivity as $d \rightarrow \infty$, i.e., the event that the robot will eventually be connected. Then, there could be cases where $P_{\text{conn},\infty} < 1$. Thus, to fully characterize the first passage statistics and embrace this possibility, we further consider $P_{\text{conn},\infty}$ as well.

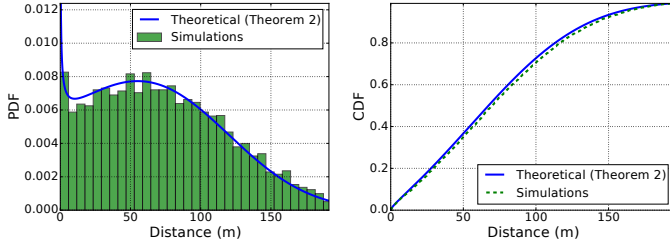


Fig. 3: Upcrossing first passage distance without multipath (left) PDF and (right) CDF for $d_{\text{src}} = 500$ m and $\theta = \pi/4$ rad.

Fig. 4, for instance, shows the contour plot of the probability of connectivity $P_{\text{conn},\infty}$, as a function of d_{src} and θ . This plot is representative of the connection statistics for a given space and given set of channel parameters. It is easy to see that the FPD statistics are identical for angle θ and $2\pi - \theta$, and thus in Fig. 4 we plot only for $\theta \in [0, \pi]$. As expected, with an increase in θ , i.e., angling away from the remote operator, $P_{\text{conn},\infty}$ decreases, i.e., there is a higher non-zero probability that the robot will never get connected. Note that for every d_{src} , there is a positive angle $\phi > 0$ for which for angle $\theta \leq \phi$, connectivity is a sure event, i.e., $P_{\text{conn},\infty} = 1$. For $\theta > \phi$, connectivity is no longer certain and $P_{\text{conn},\infty}$ begins to drop. For instance, $d_{\text{src}} = 700$ m has a ϕ of about 0.6 rad. Furthermore, as d_{src} increases, ϕ decreases as can be seen from Fig. 4, i.e., the robot needs to stay closer to $\theta = 0$ to guarantee $P_{\text{conn},\infty} = 1$.

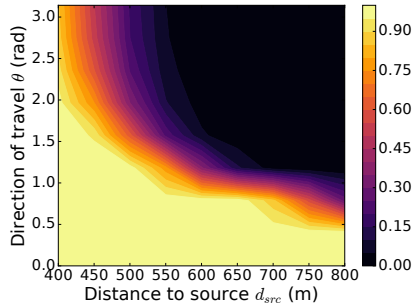


Fig. 4: Contour plot of eventual probability of connectivity $P_{\text{conn},\infty}$, without considering multipath, as a function of d_{src} and θ . Readers are referred to the color pdf for a better viewing.

Different environments will have different underlying channel parameters. Thus, we next consider the impact of the underlying channel parameters on the first passage

⁴This issue also arises in the general literature on first passage [29].

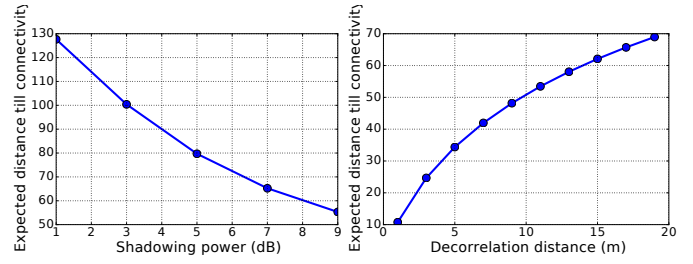


Fig. 5: Expected distance till connectivity (without multipath) as a function of (left) shadowing power, and (right) shadowing decorrelation distance, for the case of $d_{\text{src}} = 500$ m and $\theta = 0$ rad.

distance. Fig. 5 shows the expected distance traveled as a function of the shadowing decorrelation distance (β_{SH}) and the shadowing variance (σ_{SH}^2) when $d_{\text{src}} = 500$ m and $\theta = 0$ rad. Since the robot is moving towards the remote operator in this case, the probability of eventual connectivity $P_{\text{conn},\infty}$ is always 1. We next interpret the observed trends by expressing the channel power $\Gamma(d)$ as a stochastic differential equation (4). As discussed in Remark 2, the change in channel power $\Delta\Gamma(d)$ in an increment Δd , is given by a deterministic component $A(\gamma, d)\Delta d$ and a random component $B\Delta W(d)$. Increasing the shadowing power directly increases the diffusion term $B = 2\sigma^2/\beta_{\text{SH}}$, and thus increases the variance of the random component, i.e. the spatial variance of the channel power increases. Thus, with a higher probability, $\Gamma(d)$ stumbles upon the connectivity threshold earlier, resulting in a smaller first passage distance. An increase in the decorrelation distance, on the other hand, implies a greater spatial correlation of the channel power and decreases the spatial variation. Thus, we observe that the expected traveled distance increases when increasing the decorrelation distance.

B. Results When Including Multipath

In this section, we consider the case where multipath of the environment can not be neglected. We then model the multipath fading as an uncorrelated Rician random variable (in the linear domain). Rician distribution is a common distribution for characterizing multipath [15] and is given by

$$f_{\text{ric}}(z) = (1 + K_{\text{ric}})e^{-K_{\text{ric}} - (1 + K_{\text{ric}})z} I_0 \left(2\sqrt{zK_{\text{ric}}(1 + K_{\text{ric}})} \right),$$

where $I_0(\cdot)$ is the modified 0th order Bessel function and the parameter K_{ric} is the ratio of the power in the line of sight component to the power in the non-line of sight components of the channel. We take $K_{\text{ric}} = 1.59$, unless specified otherwise. The step size Δ is taken to be 0.1 m and the total distance traveled by the robot along the chosen direction is 20 m. Fig. 6 shows the PDF and CDF of the upcrossing FPD for $d_{\text{src}} = 500$ m, and with the robot moving at angle $\theta = \pi/4$ rad. The histogram obtained via brute-force simulation is also plotted for comparison. It can be seen that our derivations match the simulated ones well.

Fig. 7 shows the probability of connectivity (after traveling 20 m) as a function of K_{ric} , for $d_{\text{src}} = 500$ m and $\theta = 0$ rad. For large values of K_{ric} , the line of sight component

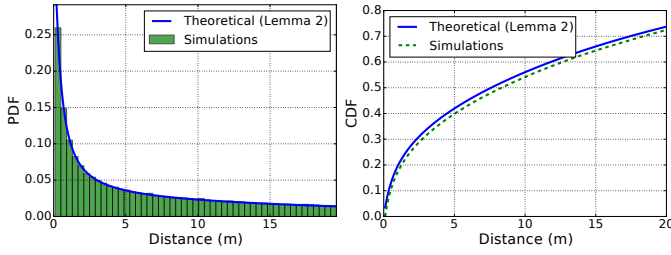


Fig. 6: Upcrossing first passage distance with multipath (left) PDF and (right) CDF for $d_{\text{src}} = 500$ m and $\theta = \pi/4$ rad.

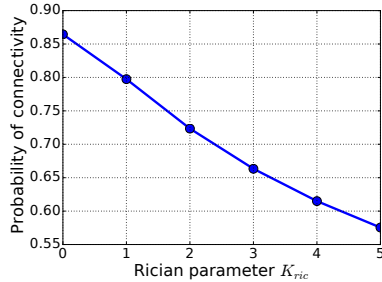


Fig. 7: Probability of connectivity after traveling 20 m when multipath is included, as a function of the Rician parameter K_{ric} , for $d_{\text{src}} = 500$ m and $\theta = 0$ rad.

dominates and results in a more deterministic multipath term. Decreasing K_{ric} , on the other hand, results in an increase in the variance of the multipath component, thus increasing the randomness of the channel. As a consequence of this, $\Gamma(d)$ would cross the connectivity threshold earlier with a higher probability (due to the increase in channel randomness).

VI. CONCLUSIONS

In this paper, we considered a robot that needs to connect to a remote human operator (or to another robot) as it moves along a path. We mathematically characterized the PDF of the first passage distance to connectivity, i.e., the PDF of the distance traveled before connectivity occurs, as a function of the underlying channel parameters. For the case where multipath is negligible, we utilized the stochastic differential equation literature to derive the PDF of the first passage distance considering shadowing and path loss components of the channel. We then included the effect of multipath and characterized the first passage distance using stochastic dynamic programming. Finally, we confirmed our theoretical derivations with several simulation results obtained with real channel parameters, and highlighted interesting trends of the first passage distance.

REFERENCES

- [1] A. Ghaffarkhah and Y. Mostofi. Path Planning for Networked Robotic Surveillance. *IEEE Transactions on Signal Processing*, 60(7):3560–3575, July 2012.
- [2] Jorge Cortes, Sonia Martinez, Timur Karatas, and Francesco Bullo. Coverage control for mobile sensing networks. In *Proceedings of IEEE International Conference on Robotics and Automation*, volume 2, pages 1327–1332. IEEE, 2002.
- [3] H. Cai and Y. Mostofi. Asking for help with the right question by predicting human visual performance. In *Proceedings of Robotics: Science and Systems*, 2016.
- [4] H. Cai and Y. Mostofi. A human-robot collaborative traveling salesman problem: Robotic site inspection with human assistance. In *Proceedings of the American Control Conference*, pages 6170–6176, July 2016.

- [5] Guy Hoffman and Cynthia Breazeal. Collaboration in human-robot teams. In *Proc. of the AIAA 1st Intelligent Systems Technical Conference, Chicago, IL, USA*, 2004.
- [6] Maria Carmela De Gennaro and Ali Jadbabaie. Decentralized control of connectivity for multi-agent systems. In *45th IEEE Conference on Decision and Control*, pages 3628–3633. IEEE, 2006.
- [7] Ethan Stump, Ali Jadbabaie, and Vijay Kumar. Connectivity management in mobile robot teams. In *IEEE International Conference on Robotics and Automation*, pages 1525–1530. IEEE, 2008.
- [8] Y. Yan and Y. Mostofi. Robotic router formation in realistic communication environments. *IEEE Transactions on Robotics*, 28(4):810–827, 2012.
- [9] Arjun Muralidharan and Yasamin Mostofi. Distributed beamforming using mobile robots. In *IEEE International Conference on Acoustics, Speech and Signal Processing (ICASSP)*, pages 6385–6389. IEEE, 2016.
- [10] Y. Yan and Y. Mostofi. To Go or Not to Go On Energy-Aware and Communication-Aware Robotic Operation. *IEEE Transactions on Control of Network Systems*, 1(3):218 – 231, July 2014.
- [11] Michael M Zavlanos, Alejandro Ribeiro, and George J Pappas. Mobility & routing control in networks of robots. In *49th IEEE Conference on Decision and Control (CDC)*, pages 7545–7550. IEEE, 2010.
- [12] Chia Ching Ooi and Christian Schindelbauer. Minimal energy path planning for wireless robots. *Mobile Networks and Applications*, 14(3):309–321, 2009.
- [13] Usman Ali, Hong Cai, Yasamin Mostofi, and Yorai Wardi. Motion and communication co-optimization with path planning and online channel prediction. In *2016 American Control Conference (ACC)*, pages 7079–7084. IEEE, 2016.
- [14] Arnold JF Siegert. On the first passage time probability problem. *Physical Review*, 81(4):617, 1951.
- [15] Andrea Goldsmith. *Wireless communications*. Cambridge university press, 2005.
- [16] H Hashemi. A study of temporal and spatial variations of the indoor radio propagation channel. In *IEEE International Symposium on Personal, Indoor and Mobile Radio Communications*, pages 127–134. IEEE, 1994.
- [17] Luigi M Ricciardi and Shunsuke Sato. First-passage-time density and moments of the ornstein-uhlenbeck process. *Journal of Applied Probability*, pages 43–57, 1988.
- [18] Luigi M Ricciardi and Laura Sacerdote. The ornstein-uhlenbeck process as a model for neuronal activity. *Biological cybernetics*, 35(1):1–9, 1979.
- [19] Boris Leblanc and Olivier Scaillet. Path dependent options on yields in the affine term structure model. *Finance and Stochastics*, 2(4):349–367, 1998.
- [20] Crispin Gardiner. *Stochastic methods*. Springer Berlin, 2009.
- [21] E Di Nardo, AG Nobile, E Pirozzi, and LM Ricciardi. A computational approach to first-passage-time problems for gauss–markov processes. *Advances in Applied Probability*, 33(2):453–482, 2001.
- [22] Richard M Dudley. *Real analysis and probability*, volume 74. Cambridge University Press, 2002.
- [23] Athanasios Papoulis and S Unnikrishna Pillai. *Probability, random variables, and stochastic processes*. Tata McGraw-Hill Education, 2002.
- [24] CB Mehr and JA McFadden. Certain properties of gaussian processes and their first-passage times. *Journal of the Royal Statistical Society. Series B (Methodological)*, pages 505–522, 1965.
- [25] Joseph L Doob. Heuristic approach to the kolmogorov-smirnov theorems. *The Annals of Mathematical Statistics*, 20(3):393–403, 1949.
- [26] Alireza Ghaffarkhah and Yasamin Mostofi. Channel learning and communication-aware motion planning in mobile networks. In *American Control Conference (ACC), 2010*, pages 5413–5420. IEEE, 2010.
- [27] Mehrzad Malmirchegini and Yasamin Mostofi. On the spatial predictability of communication channels. *IEEE Transactions on Wireless Communications*, 11(3):964–978, 2012.
- [28] William M Smith and Donald C Cox. Urban propagation modeling for wireless systems. Technical report, DTIC Document, 2004.
- [29] Donald A Darling and AJF Siegert. The first passage problem for a continuous markov process. *The Annals of Mathematical Statistics*, pages 624–639, 1953.